Worm Algorithm and Diagrammatic Monte Carlo

Boris Svistunov

University of Massachusetts, Amherst

Quantum Connections School

Högberga gård, Lidingö, June 10-22, 2019

(Pseudo-) classical representations of quantum statistics

$$Z = \mathrm{Tr}\, e^{-\beta H}, \qquad \beta = 1/T \qquad (\hbar = k_B = 1)$$

$$e^{-\beta H} \equiv e^{-\varepsilon H} e^{-\varepsilon H} \ldots e^{-\varepsilon H}$$

An extra dimension—the “imaginary time”—appears.

$$\mathrm{Tr}\, e^{-\beta H} = \left\langle \{\psi_0\} \right| e^{-\varepsilon H} \left| \{\psi_1\} \right\rangle \left\langle \{\psi_1\} \right| e^{-\varepsilon H} \left| \{\psi_2\} \right\rangle \ldots \left\langle \{\psi_m\} \right| e^{-\varepsilon H} \left| \{\psi_0\} \right\rangle$$

(a) Feynman’s path integrals: mapping onto polymers in *(d+1)* dimensions

(b) Functional integrals: mapping onto classical/grassmanian fields in *(d+1)*

(c) Some other *(d+1)*-representations along qualitatively similar lines

Feynman's path integral (worldline) representation of quantum statistics

$$Z = \mathrm{Tr}\, e^{-\beta H}$$

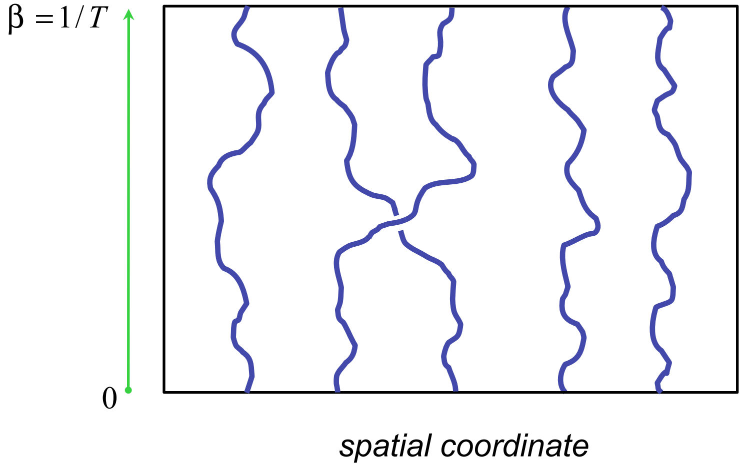

Single-particle Matsubara Green's Function

$$\hat{\Psi}_\alpha(\tau,\mathbf{r}) = e^{\tau H}\hat{\psi}_\alpha(\mathbf{r})e^{-\tau H}, \qquad \hat{\bar{\Psi}}_\alpha(\tau,\mathbf{r}) = e^{\tau H}\hat{\psi}^\dagger_\alpha(\mathbf{r})e^{-\tau H}$$

$$G_{\alpha\beta}(\tau_1,\mathbf{r}_1;\tau_2,\mathbf{r}_2) = -\langle \mathrm{T}_\tau \hat{\Psi}_\alpha(\tau_1,\mathbf{r}_1)\hat{\bar{\Psi}}_\beta(\tau_2,\mathbf{r}_2)\rangle$$

$$\langle(\ldots)\rangle \equiv Z^{-1}\,\mathrm{Tr}\,e^{-\beta H}(\ldots), \qquad Z = \mathrm{Tr}\,e^{-\beta H}$$

$$G_{\alpha\beta}(\tau_1,\mathbf{r}_1;\tau_2,\mathbf{r}_2) \equiv G_{\alpha\beta}(\tau,\mathbf{r}_1,\mathbf{r}_2), \qquad \tau = \tau_1 - \tau_2$$

$$n(\mathbf{r}) = \pm\sum_\alpha G_{\alpha\alpha}(\tau=-0,\mathbf{r},\mathbf{r}), \qquad p(\mu,T) = \int_{-\infty}^{\mu} n(\mu',T)\,d\mu'$$

↑ fermions/bosons

Two sectors of the configuration space

$$G(\mathbf{r}_1,\tau_1;\,\mathbf{r}_2,\tau_2) = \left\langle \mathrm{T}_\tau \Psi^\dagger(\mathbf{r}_2,\tau_2)\Psi(\mathbf{r}_1,\tau_1) \right\rangle = \frac{\mathrm{Tr}\,\mathrm{T}_\tau \Psi^\dagger(\mathbf{r}_2,\tau_2)\Psi(\mathbf{r}_1,\tau_1)e^{-\beta H}}{\mathrm{Tr}\,e^{-\beta H}}$$

Z-sector

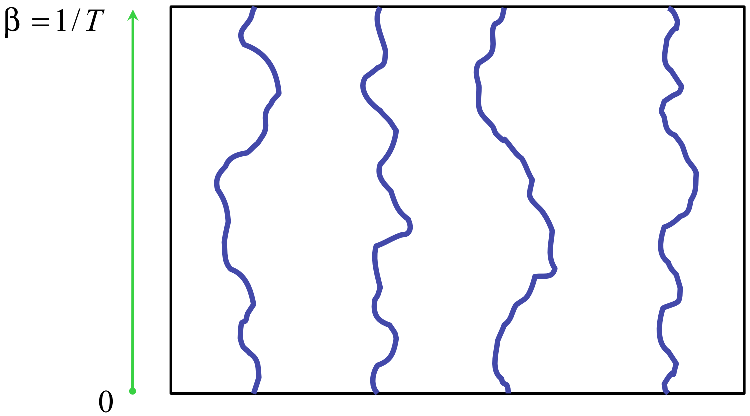

$$Z = \mathrm{Tr}\,e^{-\beta H}$$

G-sector

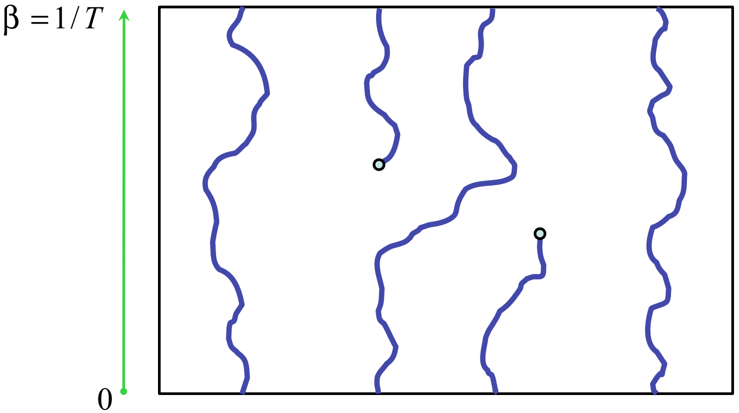

$$\mathrm{Tr}\,\mathrm{T}_\tau \Psi^\dagger(\mathbf{r}_2,\tau_2)\Psi(\mathbf{r}_1,\tau_1)e^{-\beta H}$$

By Diagrammatic Monte Carlo we mean:

1. Metropolis-Hastings-type Monte Carlo sampling of series of (similar) integrals with *variable number of integration variables*.

2. The above technique applied to *Feynman's diagrams* in the thermodynamic limit, and especially in *combination with analytic diagrammatic tricks* (e.g., Dyson's and ladder, summation, skeleton diagrams, etc.) and general re-summation techniques.

Traditional Quantum Monte Carlo:

1. Map a *d*-dimensional quantum system onto a *(d+1)*-dimensional classical counterpart.

2. Simulate the latter by Monte Carlo.

Diagrammatic Monte Carlo (DiagMC):

Samples diagrammatic series.

If applied to Feynman's diagrammatics, DiagMC simulates an answer in thermodynamic limit.

Feynman diagrams

Generic structure of diagrammatic expansions:

$$Q(y) = \sum_{m=0}^{\infty} \sum_{\xi_m} \int D(\xi_m, y, x_1, x_2, \ldots, x_m)\, dx_1\, dx_2 \cdots dx_m$$

These functions are visualized with diagrams.

Example:

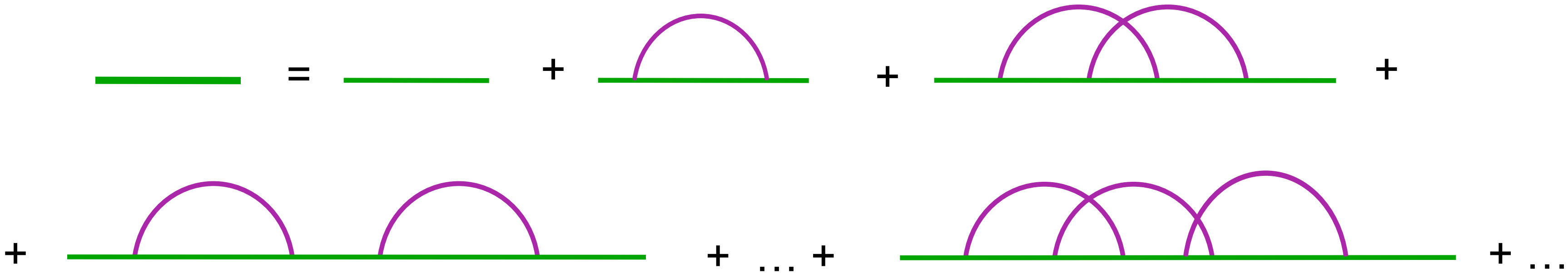

$Q(y)$ ***can be sampled by Monte Carlo***

Diagrammatic MC: Random walk in the diagrammatic space

Not to be confused with the diagram-by-diagram evaluation!

The space = diagram order + topology + internal/external continuous variables

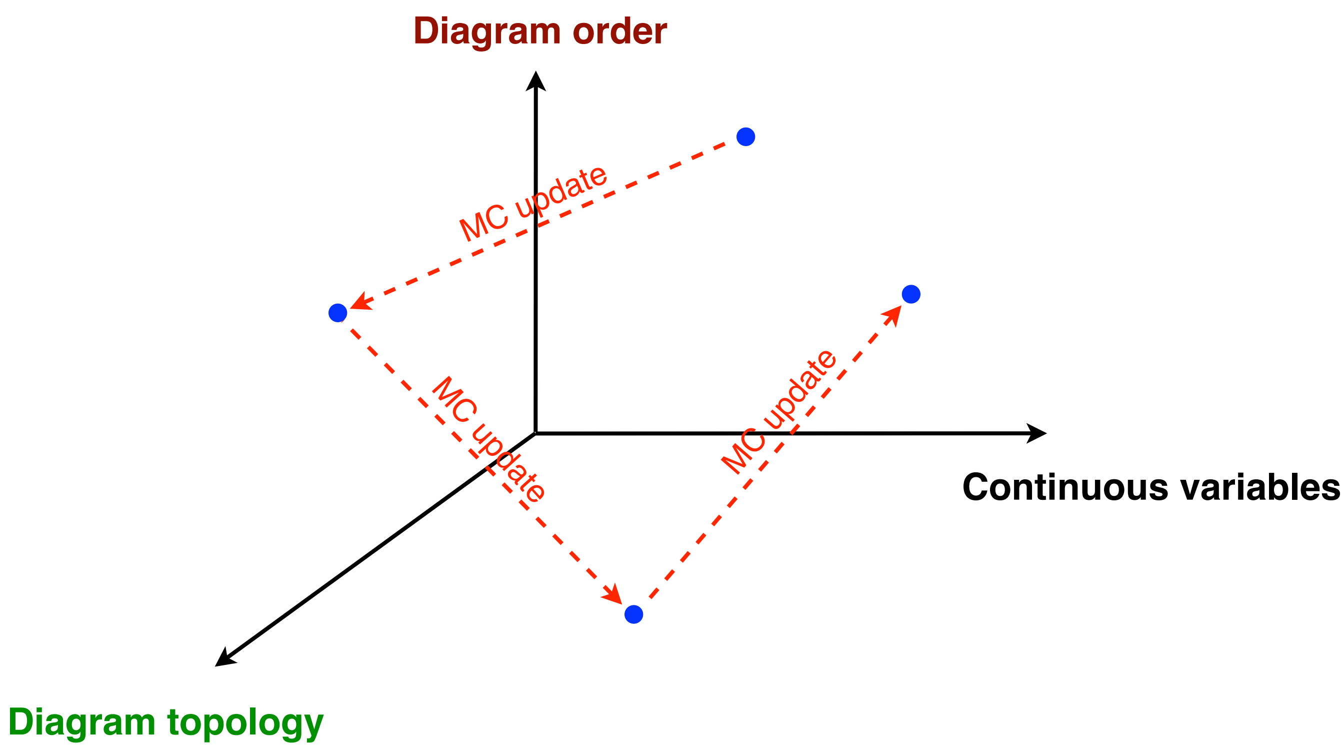

Principles of stochastic sampling

Metropolis-Hastings Algorithm

N. Metropolis, A. W. Rosenbluth, M. N. Rosenbluth, A. H. Teller, and E. Teller (1953)

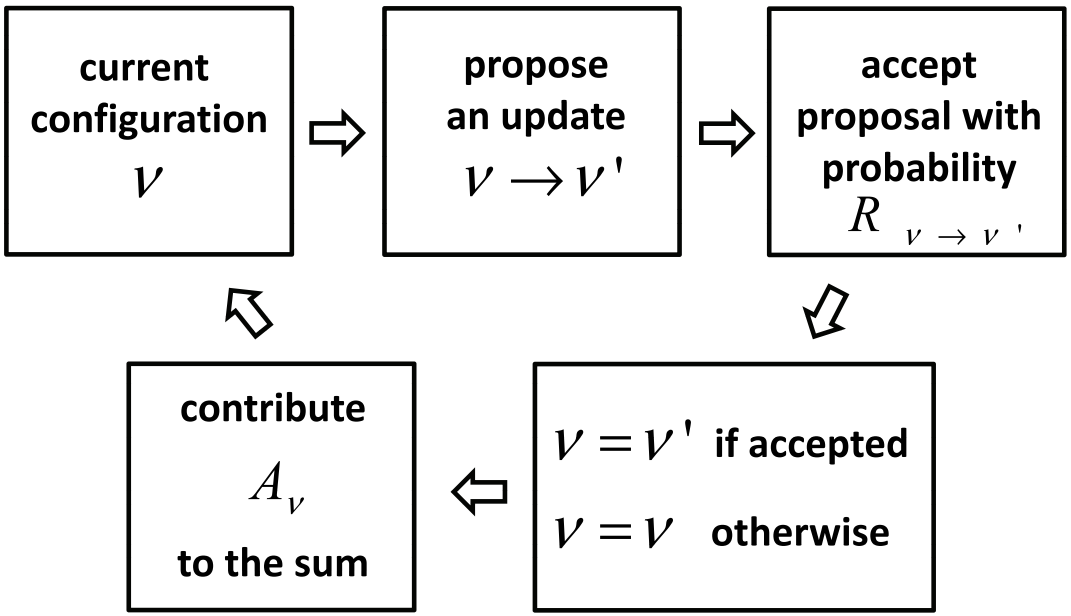

Markov-type chain of updates transforming system configurations

Balancing: Metropolis Algorithm

For details, see, e.g.: http://people.umass.edu/~bvs/Metr_alg.pdf

$$\sum_b \left(N_a P_{a\to b} - N_b P_{b\to a} \right) = 0$$ *generic balance equation for a Markovian process*

We want $\{P_{a\to b}\}$ such that: $N_a \propto W_a$.

Continuum of solutions for $\{P_{a\to b}\}$.

Confine ourselves with ***detailed balance:*** $W_a P_{a\to b} = W_b P_{b\to a}$

Still continuum of solutions for $\{P_{a\to b}\}$, *with a very natural one being:*

$$P_{a\to b} = \begin{cases} 1, & \text{if} \quad W_b \geq W_a , \\ W_b / W_a , & \text{if} \quad W_b < W_a . \end{cases}$$

Metropolis-Hastings Algorithm

$$W_a P_{a\to b} = W_b P_{b\to a}$$

$$P_{a\to b} = P_{a\to b}^{(propose)} P_{a\to b}^{(accept)}$$

$$W_a P_{a\to b}^{(propose)} P_{a\to b}^{(accept)} = W_b P_{b\to a}^{(propose)} P_{b\to a}^{(accept)}$$

$$P_{a\to b}^{(accept)} = \begin{cases} 1, & \text{if} \quad R_{a\to b} \geq 1, \\ R_{a\to b}, & \text{if} \quad R_{a\to b} < 1, \end{cases}$$

$$R_{a\to b} = \frac{W_b P_{b\to a}^{(propose)}}{W_a P_{a\to b}^{(propose)}}$$

The updates related to changing the number of continuous variables always come as (complementary) pairs A-B. Update A involves creating new variables, and update B involves eliminating them. For update A, the proposal probability is a product of probability $p_A^{(addr)}$ *to address the update A and the probability* $\Omega\left(\vec{X}\right)d\vec{X}$ *to seed the new variables in a given element of corresponding space.*

Here $\Omega\left(\vec{X}\right)$ *is an* ***arbitrary*** *distribution function for generating particular values of new continuous variables in the update A .*

Acceptance ratios for the updates A and B

$$R_A\left(\vec{X}\right) = \frac{New\ Diagram}{Old\ Diagram}\,\frac{p_B^{(addr)}}{p_A^{(addr)}}\,\frac{1}{\Omega\left(\vec{X}\right)}$$

$$R_B\left(\vec{X}\right) = \frac{New\ Diagram}{Old\ Diagram}\,\frac{p_A^{(addr)}}{p_B^{(addr)}}\,\Omega\left(\vec{X}\right)$$

For a tutorial, see:

http://people.umass.edu/~bvs/Metropolis_walk.pdf

http://people.umass.edu/~bvs/Scattering_length.pdf

Diagrammatic Monte Carlo for fermions:
Sign blessing rather than sign problem.

DiagMC simulates the answer in thermodynamic limit rather than a *(d+1)*-dimensional object.

Q. How can a series with *factorially* growing number of diagrams within a given order converge?

A. *Fermionic sign blessing*: Factorially accurate cancellation of different diagrams within a given order.

But why should we expect the sign blessing ?…

… Because of the absence of Dyson's collapse (for discrete and some other special systems).

Dyson's collapse

Dyson's argument (1952): *A perturbative series has* ***zero convergence radius*** *if changing the sign of interaction renders the system pathological.*

A conjecture: ***Finite convergence radius if no Dyson's collapse.***

Pauli principle protects lattice and momentum-truncated fermions from Dyson's collapse.

Q. Why necessarily fermions—how about, say, spins (also protected from collapse)?

A. For Feynman diagrammatics, we need Gaussian non-perturbed action. That’s why fermions and fermionization.

More generally, Grassmannization.

Looks like one can fermionize/Grassmannize essentially any lattice system!

Pollet, Kiselev, Prokof'ev, and Svistunov, New J. Phys. 18, 113025 (2016)

Computational complexity of diagrammatic Monte Carlo

Rossi, Prokof'ev, Svistunov, Van Houcke, and Werner, EPL 118, 10004 (2017)

$t(\varepsilon)$ the computational time needed to achieve the relative accuracy ε

$t(\varepsilon) \sim \varepsilon^{-\# \ln(\ln \varepsilon^{-1})}$ with standard DiagMC: ***quasi-polynomial***

$t(\varepsilon) \sim \varepsilon^{-\alpha}$ with Rossi's determinant trick: ***polynomial***

Rossi, PRL, 119, 045701 (2017)

Diagrammatic Monte Carlo for fermions:
Illustrative results

Model of Resonant Fermions

(from ultra-cold atoms to neutron stars)

Works whenever $R_0 \ll 1/c$ *, where* R_0 *is the range of interaction.*

No explicit interactions—just the boundary conditions:

$$\forall i,j \quad \text{at} \quad \left|\mathbf{r}_{\uparrow_i} - \mathbf{r}_{\downarrow_j}\right| \to 0: \qquad \Psi\left(\mathbf{r}_{\uparrow 1},\ldots,\mathbf{r}_{\uparrow N},\mathbf{r}_{\downarrow 1},\ldots,\mathbf{r}_{\downarrow N}\right) \to \frac{A}{\left|\mathbf{r}_{\uparrow_i} - \mathbf{r}_{\downarrow_j}\right|} + B, \qquad \frac{B}{A} = c = \text{const}$$

(In the two-body problem, the parameter c defines the s-scattering length: a = -1/c .)

$$c \gg n^{1/3} \sim k_F \quad \Rightarrow$$ BCS regime

$$-c \gg n^{1/3} \sim k_F \quad \Rightarrow$$ BEC regime

$$|c| \sim n^{1/3} \sim k_F \quad \Rightarrow$$ the crossover

$$c = 0 \quad \Rightarrow$$ unitarity point: scale invariance

Resonant fermipolaron

One (spin-down) particle interacting resonantly with an ideal (spin-up) Fermi sea.

The ground state:

A polaron, or a molecule (bound spin-up + spin-down state)

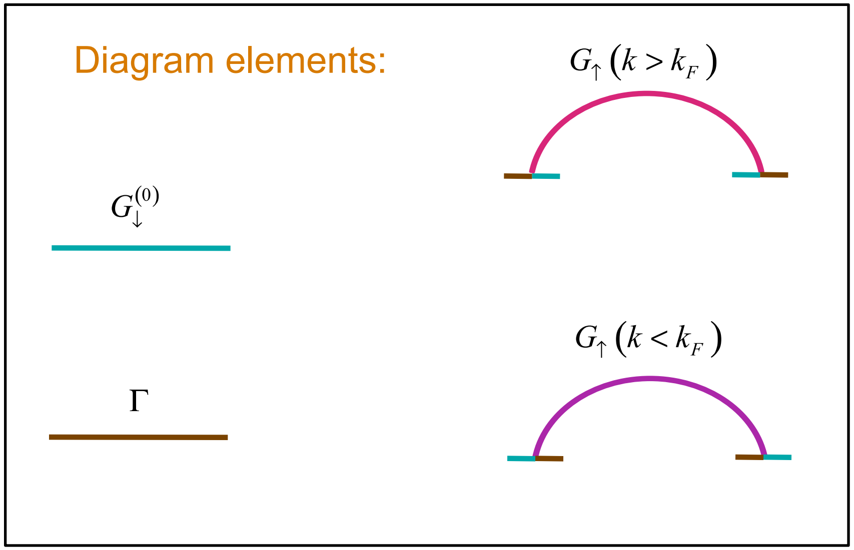

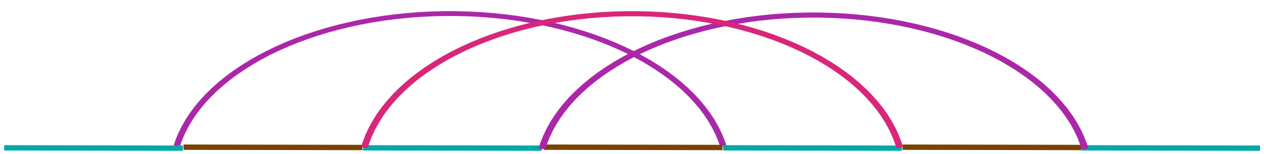

a polaron diagram

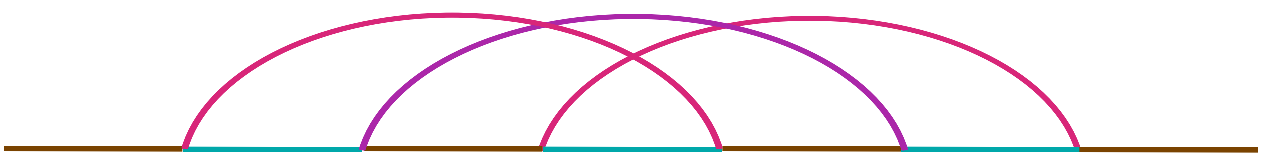

a molecule diagram

Resonant Fermi polaron: energy and effective mass

Energy

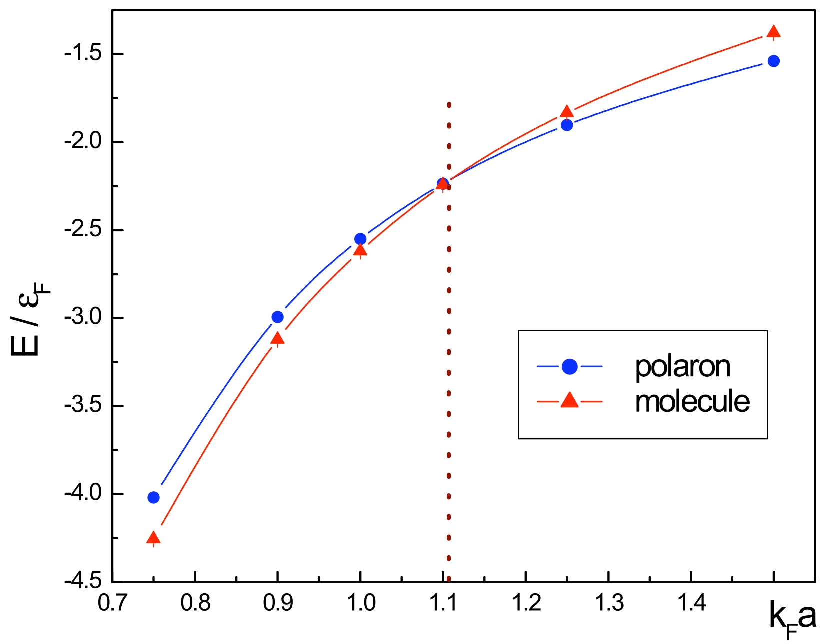

Effective Mass

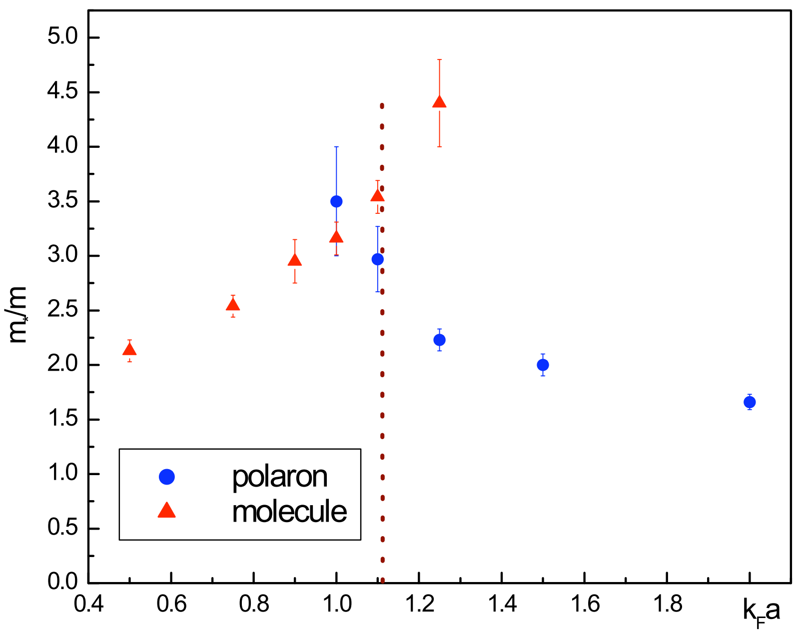

Prokof'ev and BS, 2008

Unitary Fermi gas: Number density equation of state

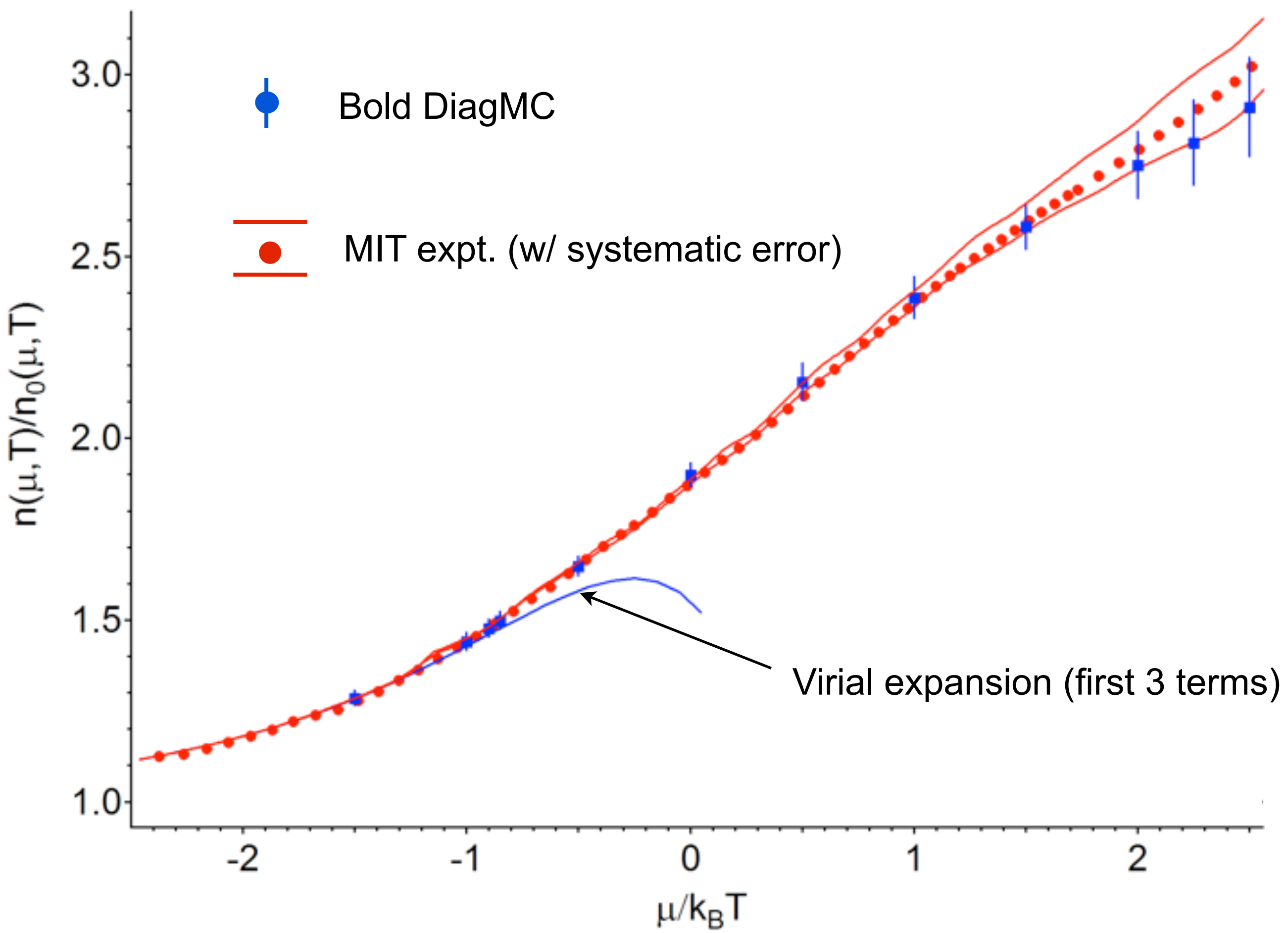

K. Van Houcke, F. Werner, E. Kozik, N. Prokofev, B. Svistunov, M. Ku, A. Sommer, L. W. Cheuk, A. Schirotzek, and M. W. Zwierlein, Nat. Phys. 8, 366 (2012); R. Rossi, T. Ohgoe, K. Van Houcke, and F. Werner, PRL 121, 130405 (2018).

Unitary Fermi gas: Momentum distribution and contact

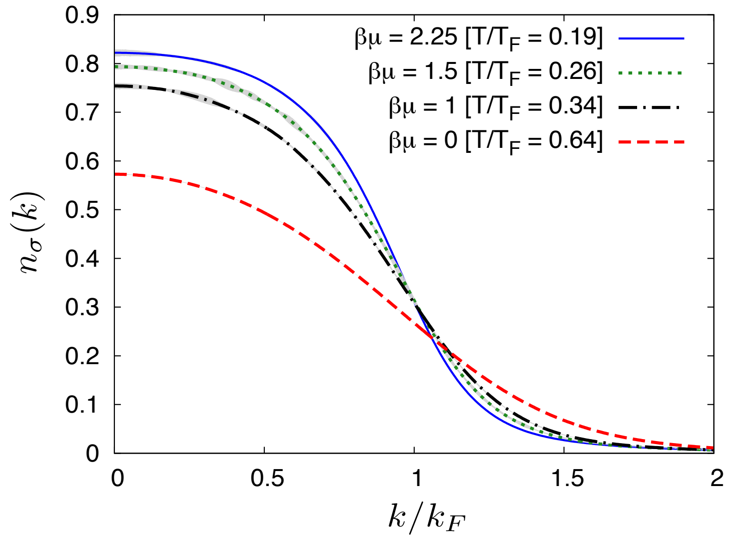

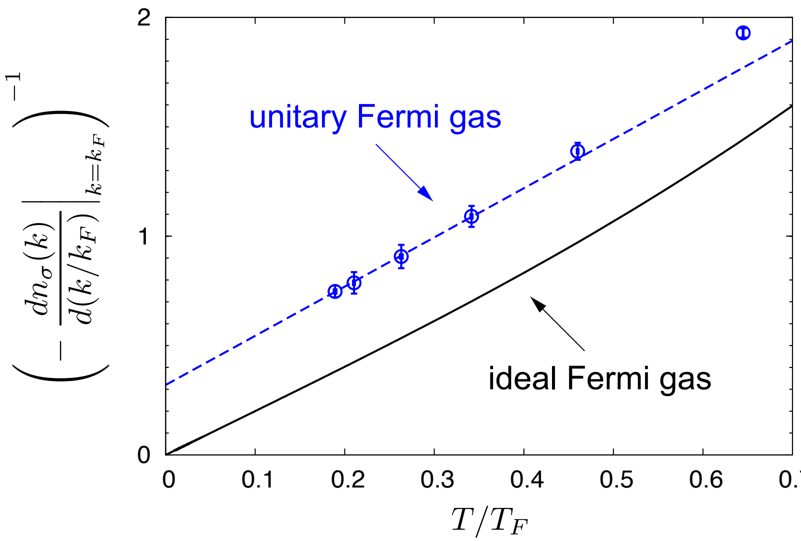

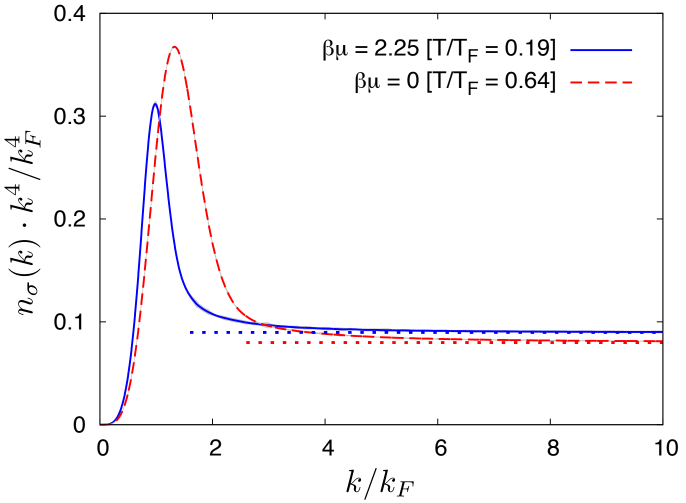

T. Ohgoe, R. Rossi, E. Kozik, N. Prokof'ev, B. Svistunov, K. Van Houcke, and F. Werner, PRL 121, 130406 (2018)

Ground-State Phase Diagram of 2D Fermi-Hubbard Model in the Emergent BCS Regime

$$H = -t \sum_{\substack{<ij> \\ \sigma=\uparrow,\downarrow}} a^{+}_{\sigma i}\, a_{\sigma j} + U \sum_{i} n_{\uparrow i}\, n_{\downarrow i}\,, \qquad n_{\sigma i} = a^{+}_{\sigma i} a_{\sigma i}$$

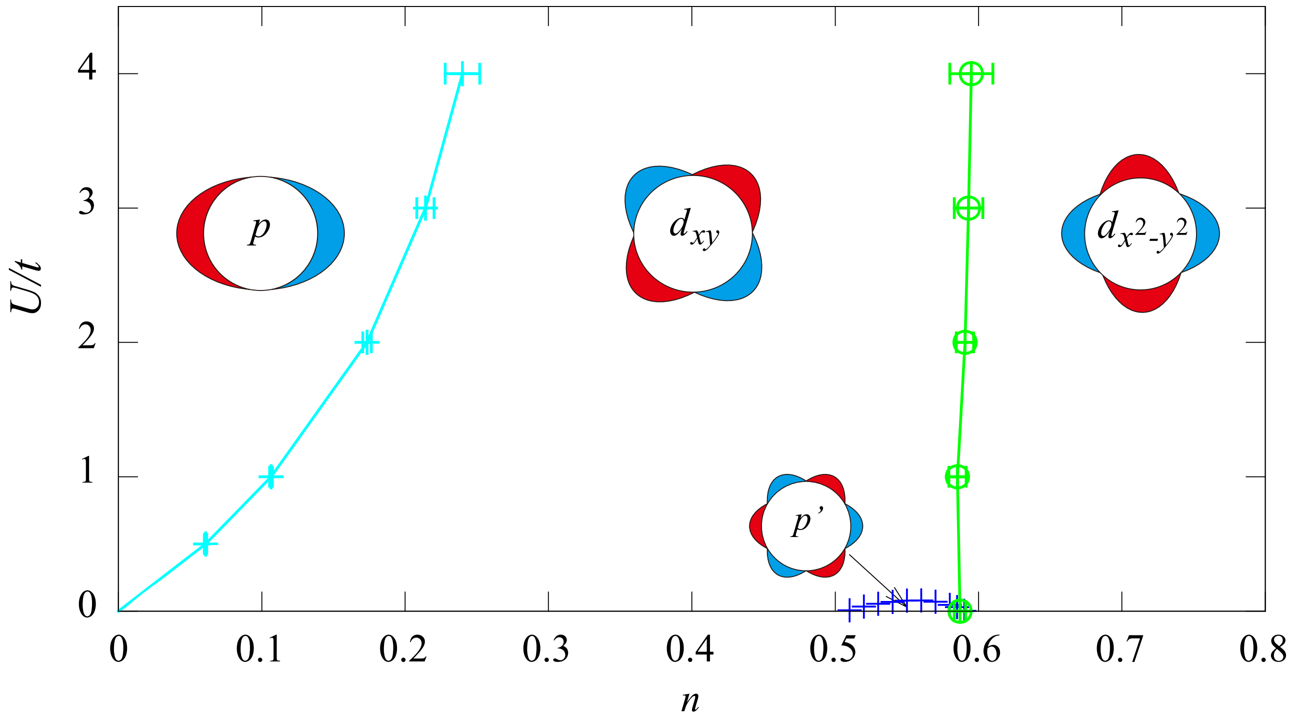

Youjin Deng, Evgeny Kozik, N. Prokof’ev and B.Svistunov, EPL **110**, 57001 (2015)

Extended crossover from Fermi liquid to quasi-antiferromagnet in the half-filled 2D Hubbard model

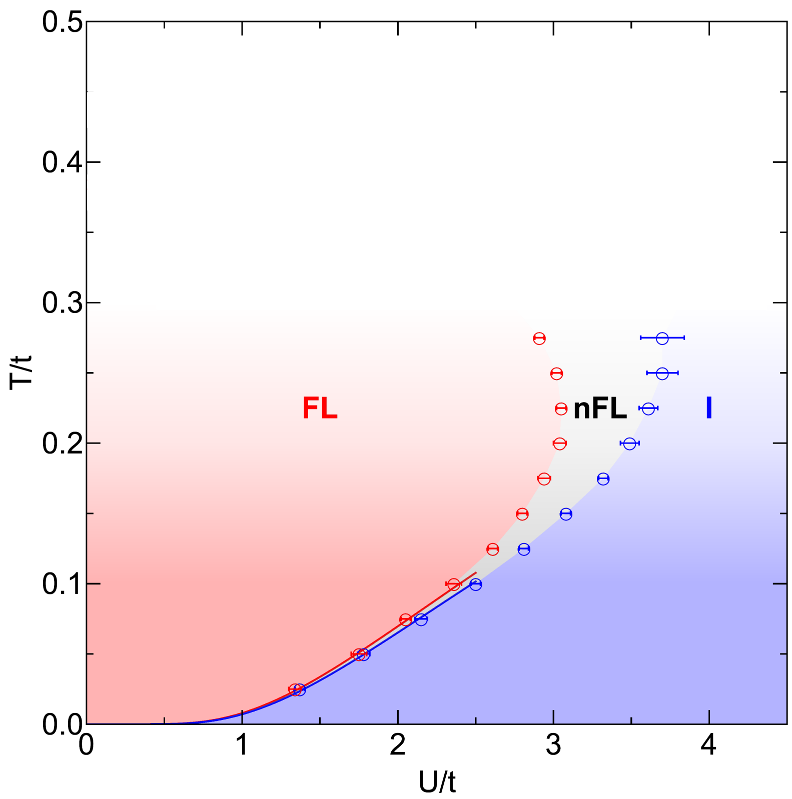

F. Simkovic, J. P. F. LeBlanc, A. J. Kim, Y. Deng, N. V. Prokof'ev, B. V. Svistunov, and E. Kozik, arXiv:1812.11503

Graphene-type systems: RG flow in Dirac liquids

Effective Coulomb coupling constant in 2D: $\alpha[l]=e^2/v_F$ **Q: How** α ***[l=ln(L)]* renormalizes with the scale of distance *l=ln(L/a)*?**

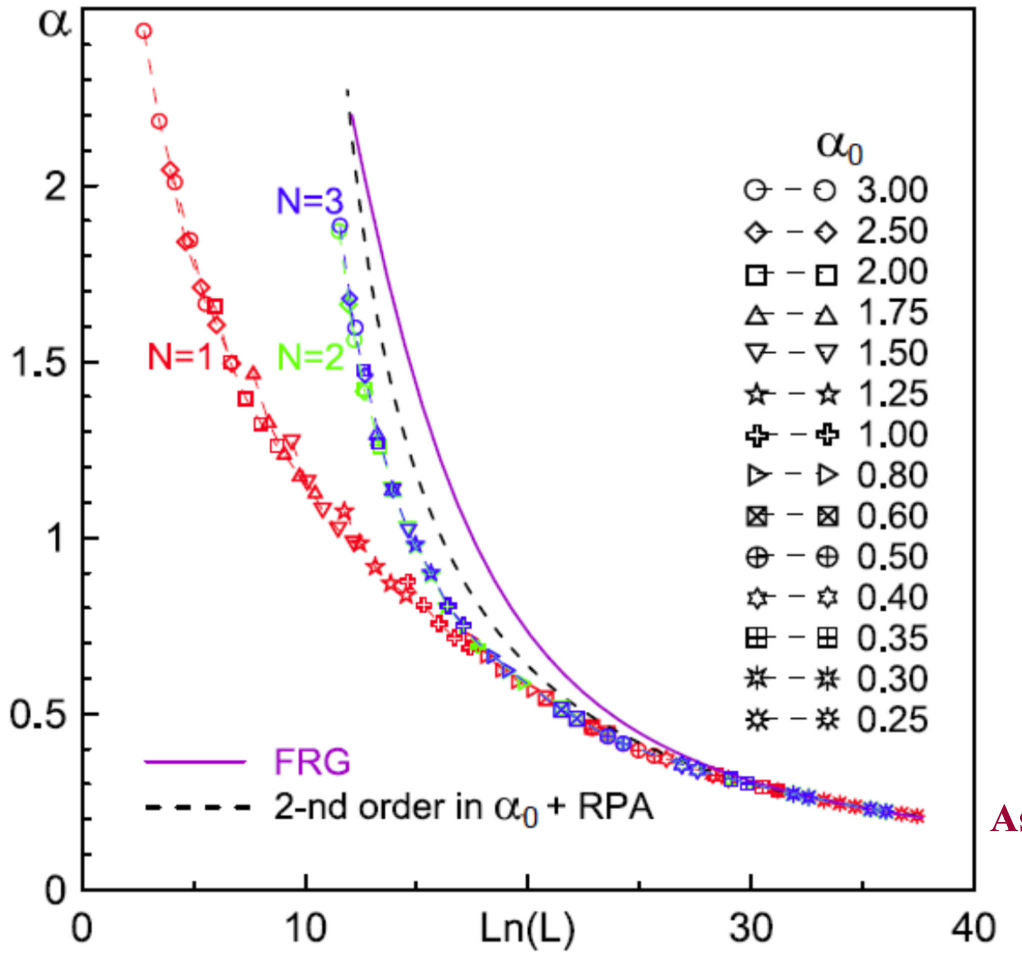

Asymptotic freedom

I.S. Tupitsyn and N.V. Prokof'ev, **Phys. Rev. Lett. 118**, 026403 (2017)

Conclusion: In the infrared limit, the system is asymptotically free with divergent Fermi velocity.

Interacting topological materials: Phase diagram of the Haldane-Hubbard-Coulomb model

Haldane-Hubbard model

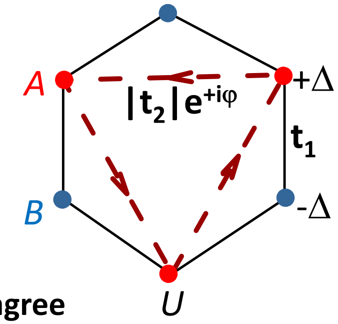

Approximate and finite-size methods strongly disagree

(T.I. Vanhala et al, PRL 116, 225305 (2016))

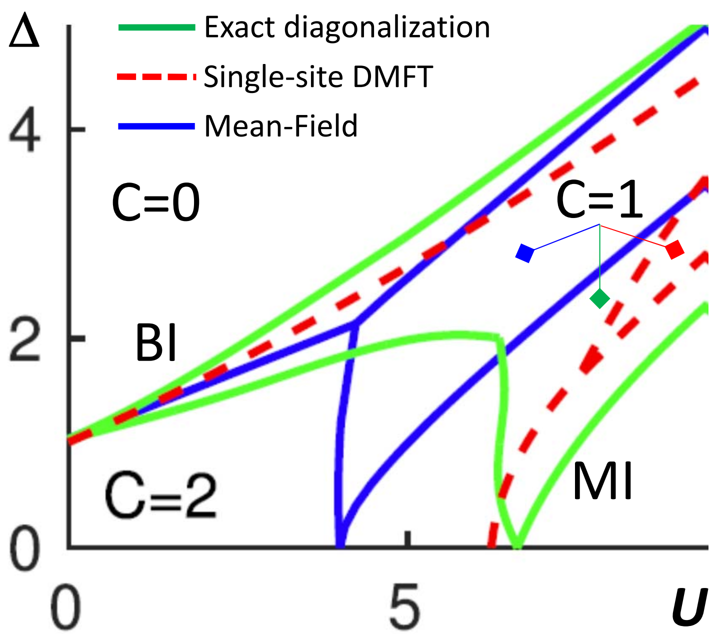

Diagrammatic result

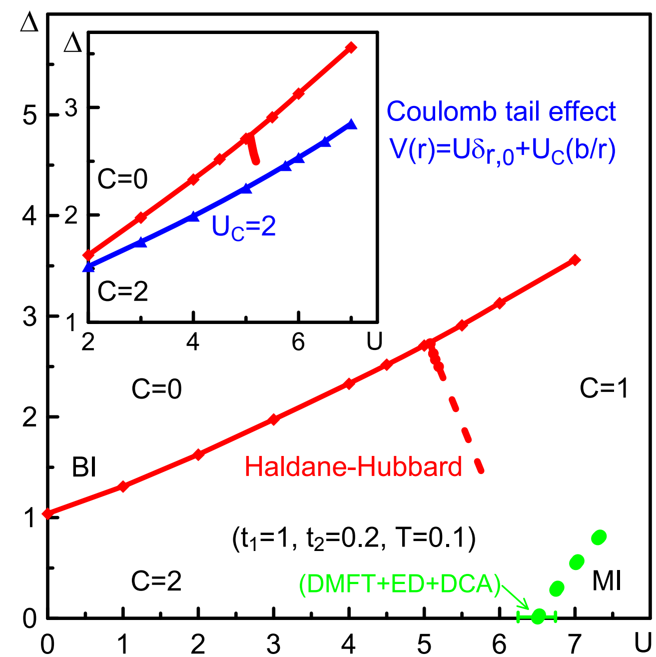

I.S. Tupitsyn and N.V. Prokof'ev, PRB 99, 121113(R) (2019)

Fermionized spins

Popov-Fedotov fermionization trick

Heisenberg model $$H = J\sum_{\langle ij\rangle} \vec{S}_i \cdot \vec{S}_j$$

Dynamical--but not statistical--equivalent $$H' = J\sum_{\langle ij\rangle}\left(f^{\dagger}_{i\alpha}\vec{\sigma}_{\alpha\beta}f_{i\beta}\right)\cdot\left(f^{\dagger}_{j\gamma}\vec{\sigma}_{\gamma\delta}f_{j\delta}\right)$$

Dynamical and statistical equivalent

$$H_{PF} = J\sum_{\langle ij\rangle}\left(f^{\dagger}_{i\alpha}\vec{\sigma}_{\alpha\beta}f_{i\beta}\right)\cdot\left(f^{\dagger}_{j\gamma}\vec{\sigma}_{\gamma\delta}f_{j\delta}\right) - \mu\sum_{j\alpha}\left(n_{j\alpha}-1\right), \qquad \mu = i\pi T/2$$

Spin-1/2 on triangular lattice by BDMC

Kulagin, Prokof'ev, Starykh, BS, and Varney, PRL**110**, 070601 (2013); PRB **87**, 024407 (2013).

Static magnetic response

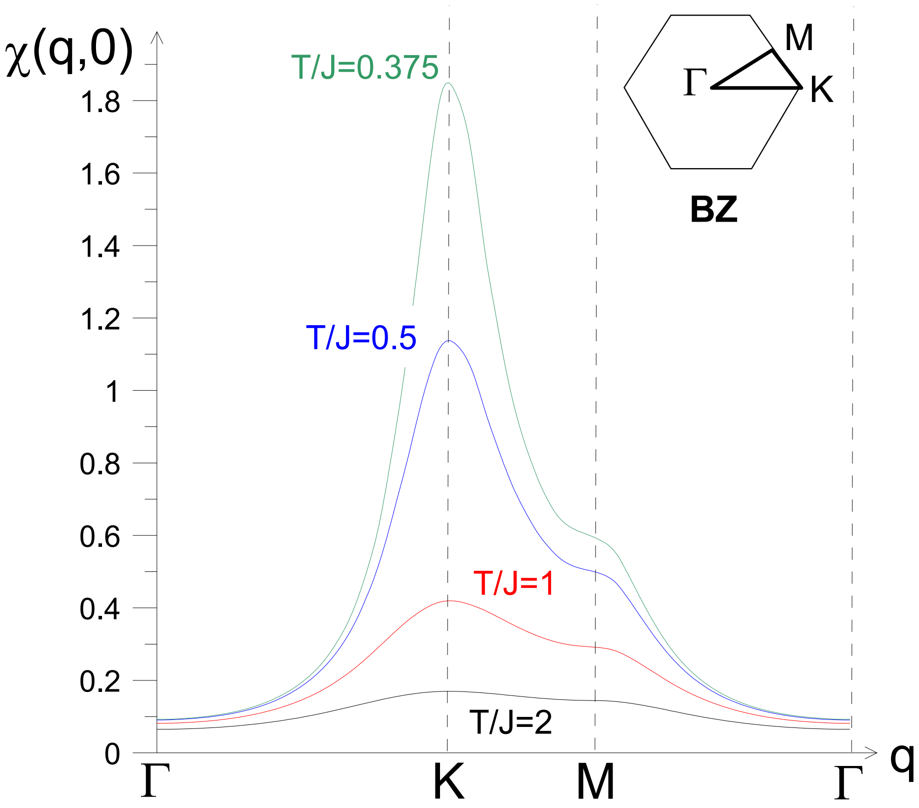

Quantum-to-classical correspondence of the static magnetic response

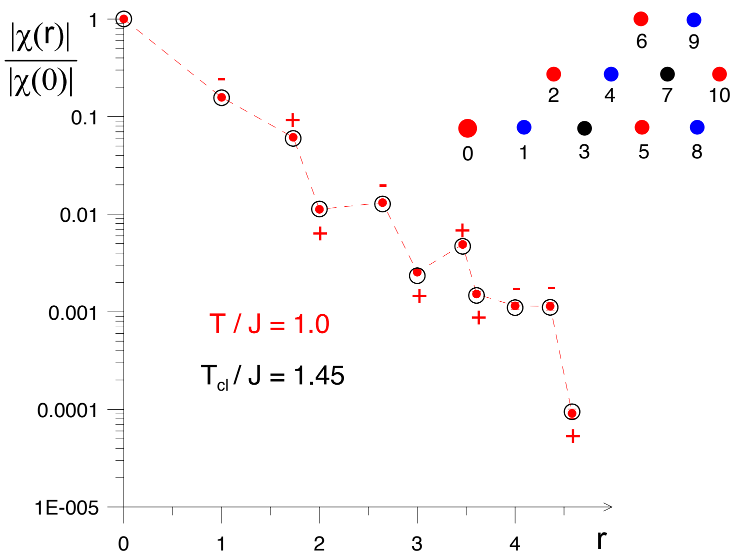

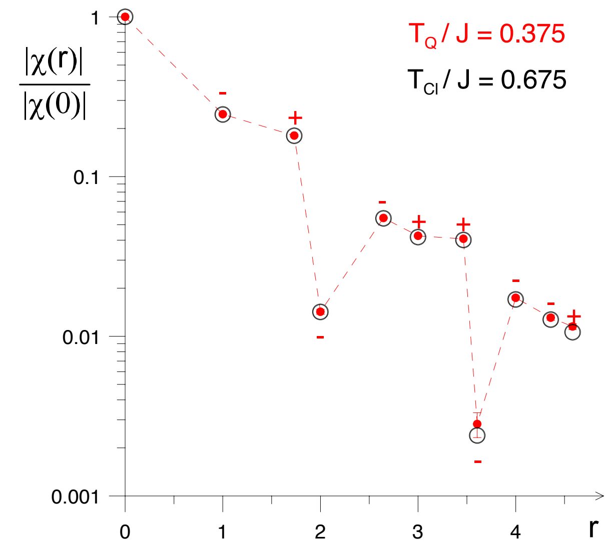

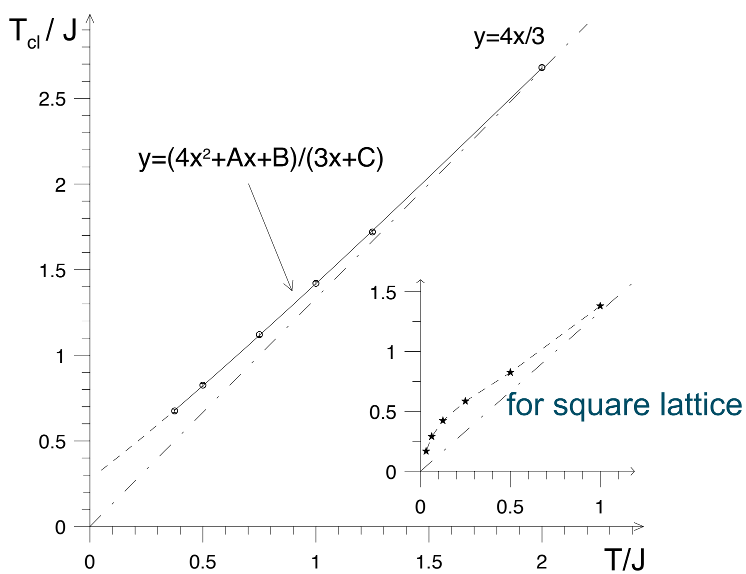

Quantum-to-classical correspondence in the Heisenberg model on kagome lattice

$T_Q/J = 1$

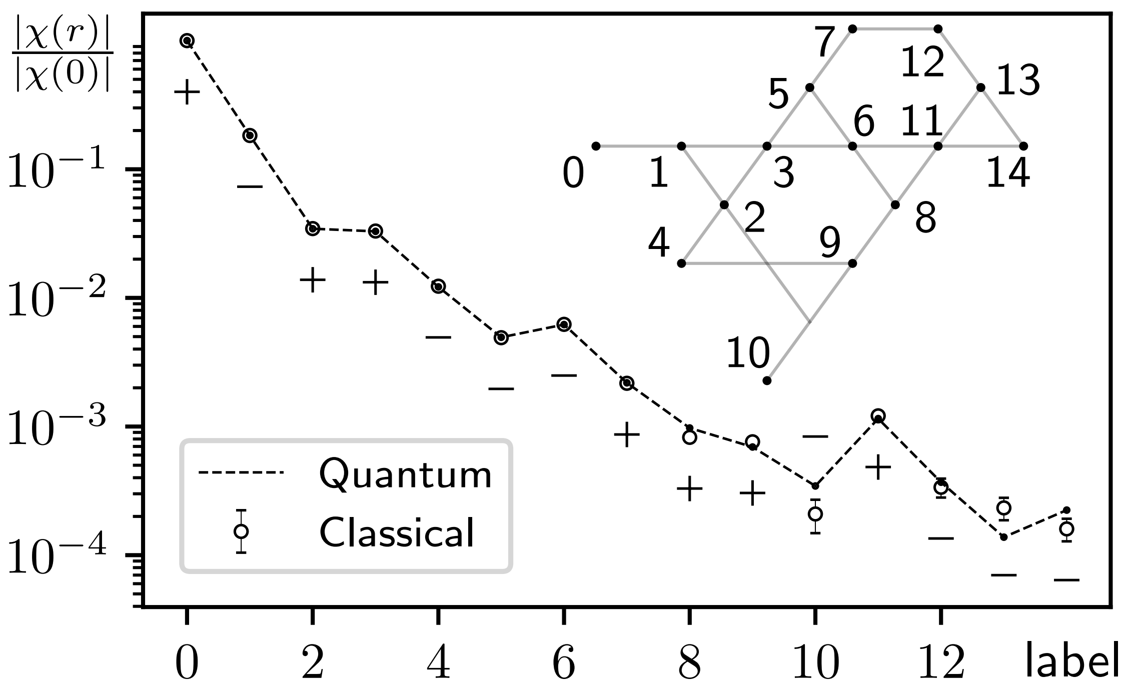

Tao Wang, Xiansheng Cai, K. Chen, N. V. Prokof'ev, and B. V. Svistunov, arXiv:1904.10081.

Worm Algorithm

Feynman's path integral (worldline) representation of quantum statistics

$$Z = \mathrm{Tr}\, e^{-\beta H}$$

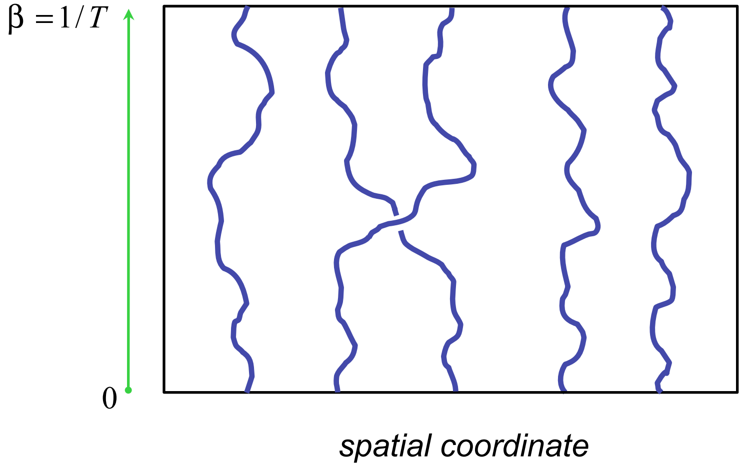

Worldline winding numbers and superfluidity

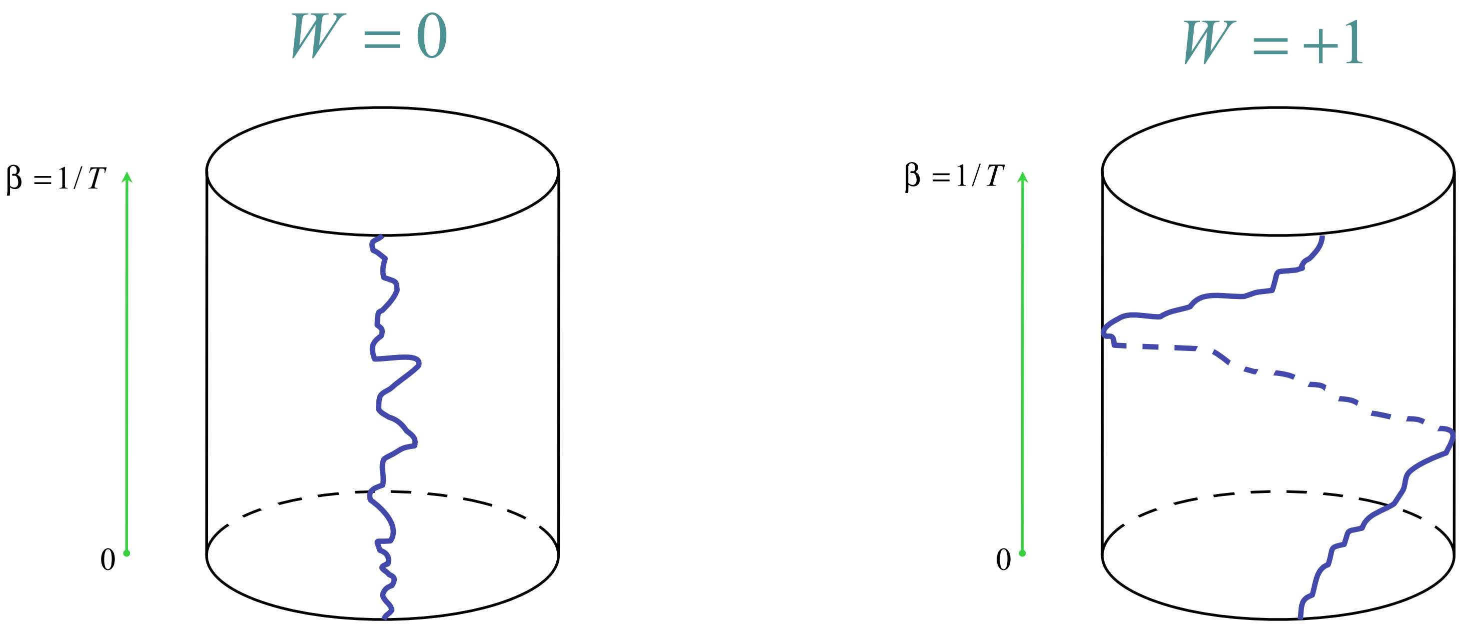

superfluid density: $$\rho_S \propto \langle W^2 \rangle / \beta L^{d-2}$$

Pollock and Ceperley, PRB 36, 8343 (1987).

Two sectors of the configuration space

$$G(\mathbf{r}_1,\tau_1;\,\mathbf{r}_2,\tau_2) = \left\langle \mathrm{T}_\tau \Psi^\dagger(\mathbf{r}_2,\tau_2)\Psi(\mathbf{r}_1,\tau_1) \right\rangle = \frac{\mathrm{Tr}\,\mathrm{T}_\tau \Psi^\dagger(\mathbf{r}_2,\tau_2)\Psi(\mathbf{r}_1,\tau_1)e^{-\beta H}}{\mathrm{Tr}\,e^{-\beta H}}$$

Z-sector

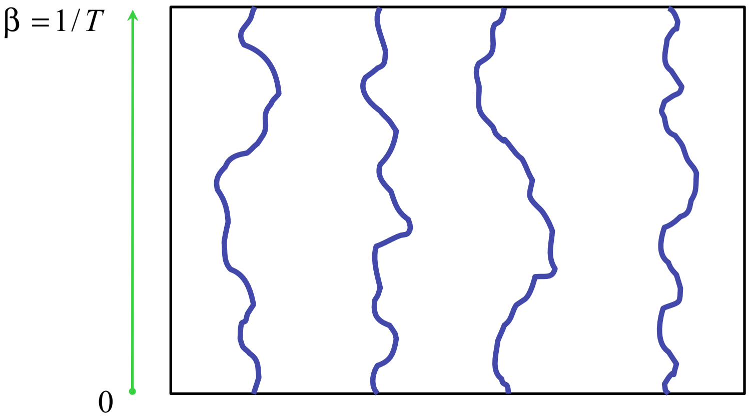

G-sector

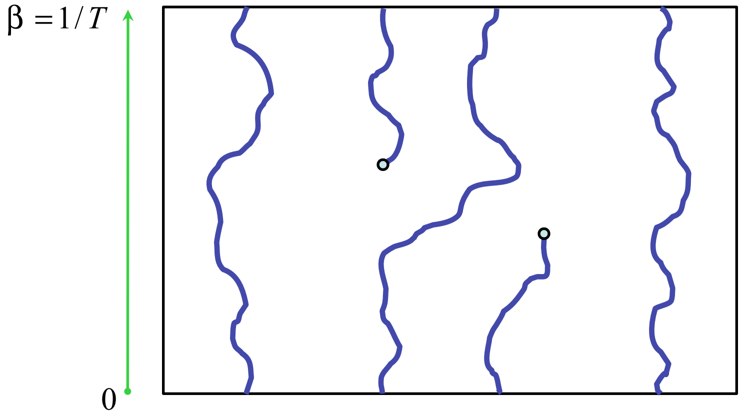

$$Z = \mathrm{Tr}\,e^{-\beta H}$$

$$\mathrm{Tr}\,\mathrm{T}_\tau \Psi^\dagger(\mathbf{r}_2,\tau_2)\Psi(\mathbf{r}_1,\tau_1)e^{-\beta H}$$

Worm algorithm: the idea

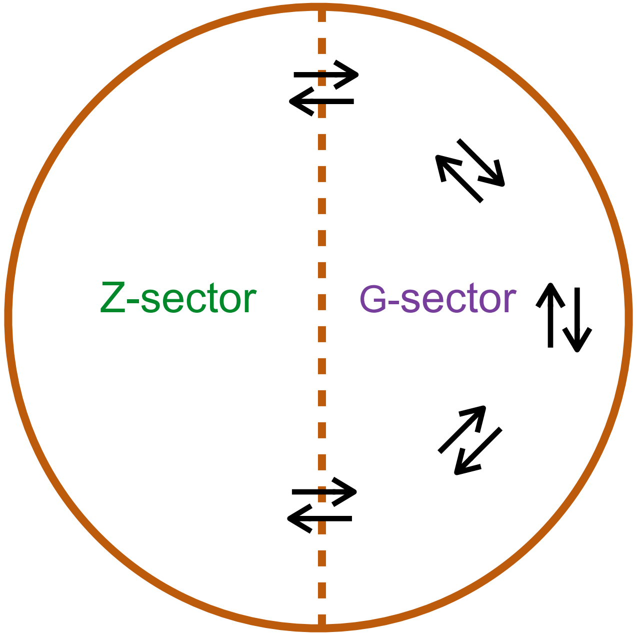

1. Combine both sectors into a single configuration space.

2. Use G-sector for efficient updates.

Prokof'ev, Svistunov, and Tupitsyn, JETP **87**, 310 (1998)

Worm algorithm updates

Prokof'ev, Svistunov, and Tupitsyn, JETP **87**, 310 (1998) *[worm for lattice models]*

Prokof'ev and Svistunov, PRL **87**, 160601 (2001) *[worm for classical models]*

Boninsegni, Prokof'ev, and Svistunov, PRL **96**, 070601 (2006) *[worm for continuous space]*

For a pedagogic introduction see:

Svistunov, Babaev, and Prokof'ev, ***Superfluid States of Matter***, Taylor & Francis, 2015.

Prokof'ev and B. Svistunov, *Worm Algorithm for Problems of Quantum and Classical Statistics*, chapter in the book: **Understanding Quantum Phase Transitions**, edited by L. D. Carr, Taylor & Francis, 2010.

Inserting/removing a short worldline piece

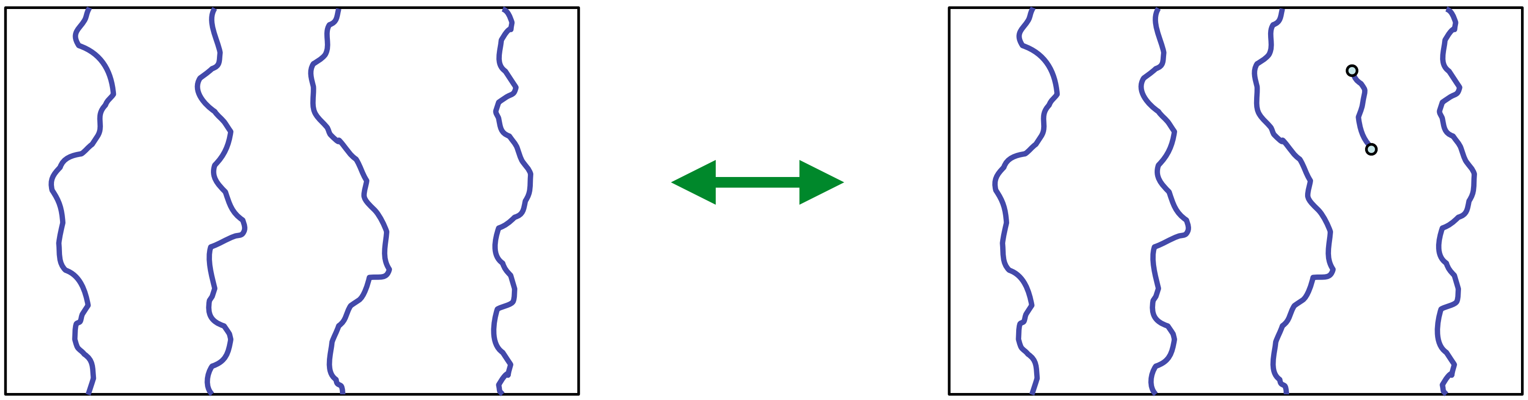

Opening/closing a worldline gap

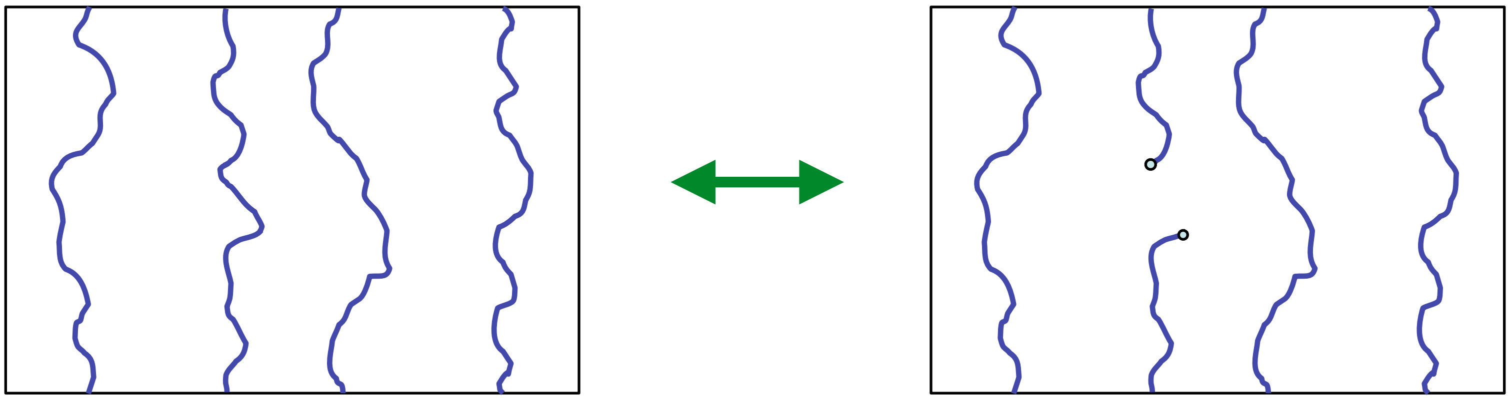

Shifting the worm

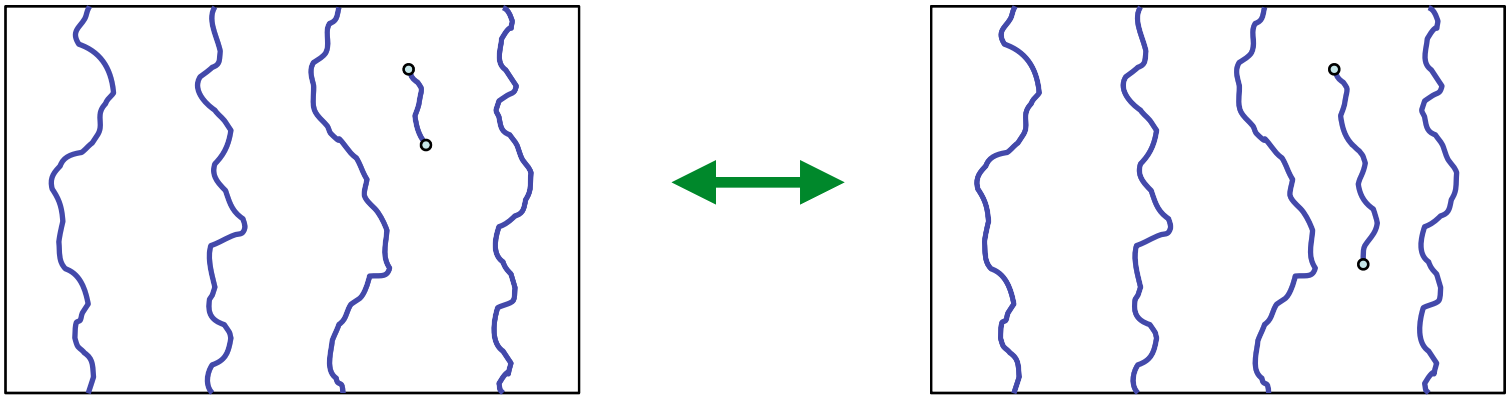

Reconnection: the most efficient update

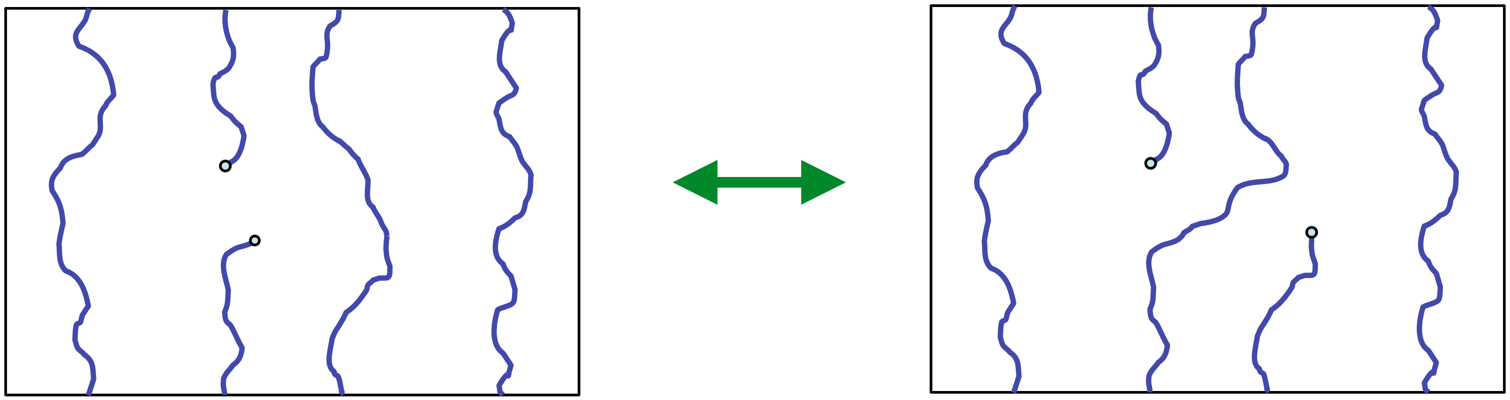

Instructive fact:

The (generic) worm algorithm for Ising-type models in 3D overperforms system-specific cluster algorithms.

Worm algorithm: illustrative applications

Superfluidity in the core of a screw dislocation in He-4 crystal

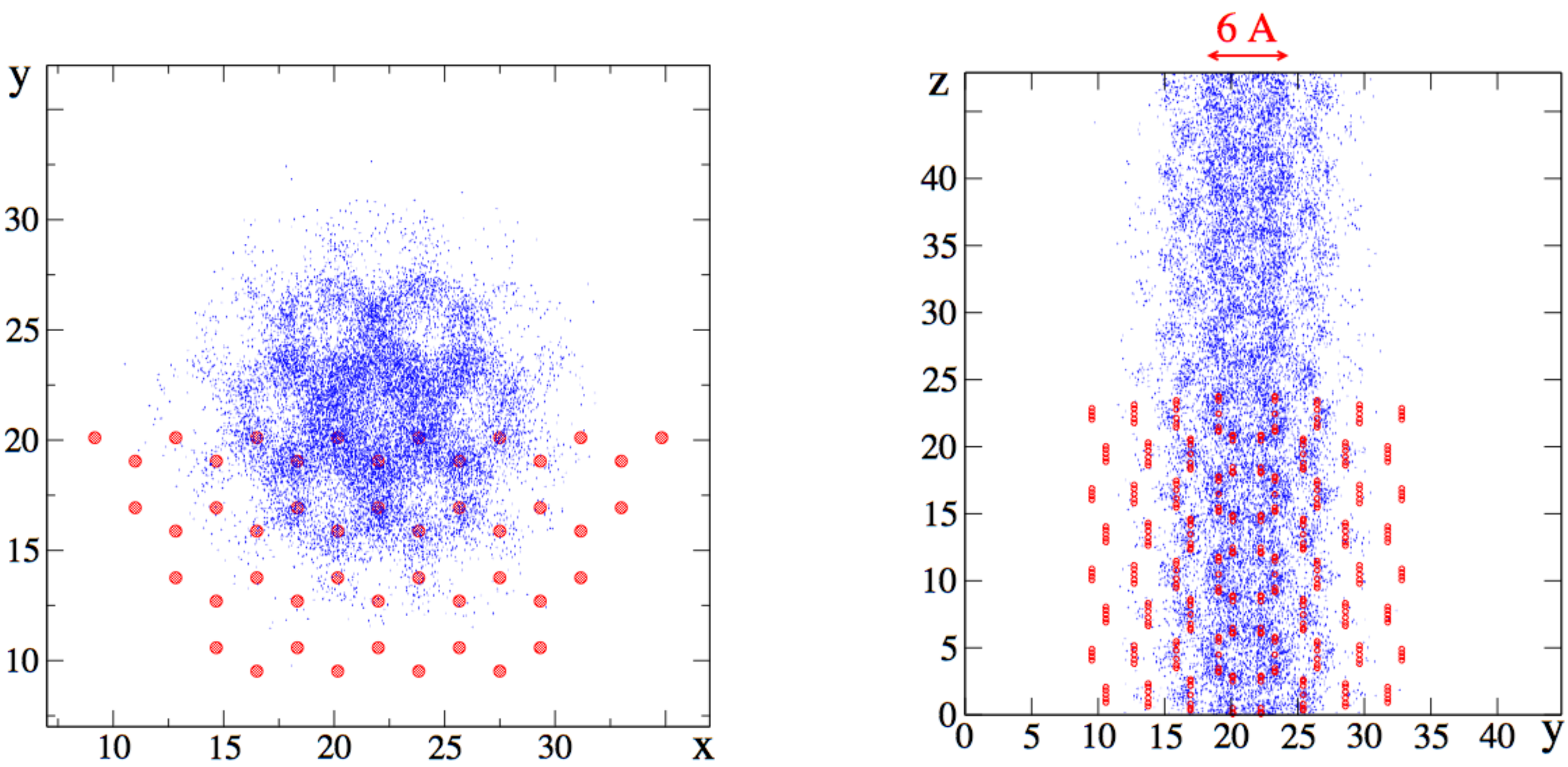

Boninsegni, Kuklov, Pollet, Prokof’ev, Svistunov, and Troyer, PRL **99**, 035301 (2007)

Robert Hallock's UMass Sandwich

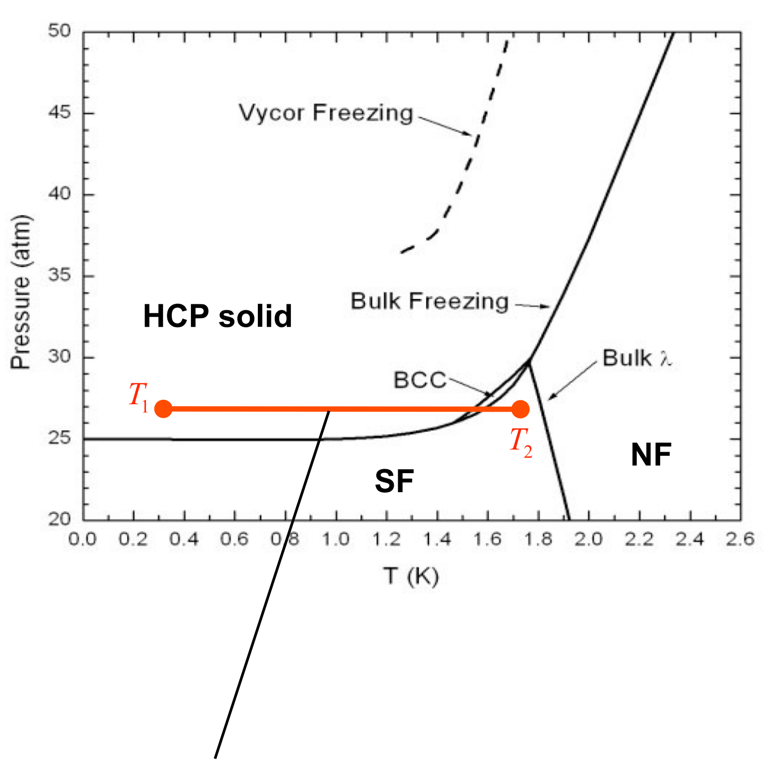

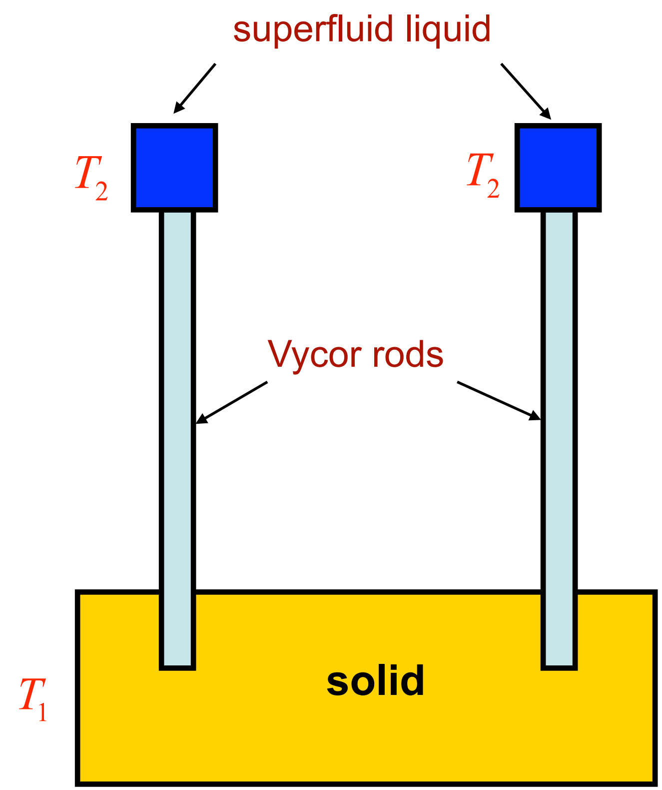

Temperature gradient in Vycor rods does the job!

For a review, see: "Is Solid Helium Supersolid" by R. Hallock in *Physics Today*, May 2015.

PRL **100,** 235301 (2008) PHYSICAL REVIEW LETTERS week ending 13 JUNE 2008

Observation of Unusual Mass Transport in Solid hcp ^{4}He

M. W. Ray and R. B. Hallock

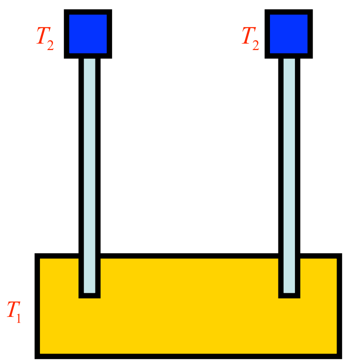

UMass sandwich

discovery:

isochoric compressibility (aka syringe effect)

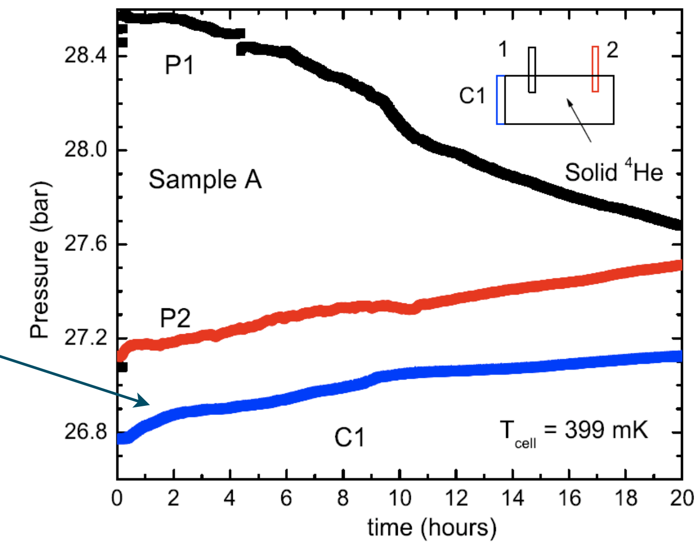

theory

PRL **103,** 175301 (2009) PHYSICAL REVIEW LETTERS week ending 23 OCTOBER 2009

Underlying Mechanism for the Giant Isochoric Compressibility of Solid ^{4}He: Superclimb of Dislocations

Ş. G. Söyler,[1] A. B. Kuklov,[2] L. Pollet,[3] N. V. Prokof'ev,[1,4] and B. V. Svistunov[1,4]

First validation of optical-lattice quantum emulator

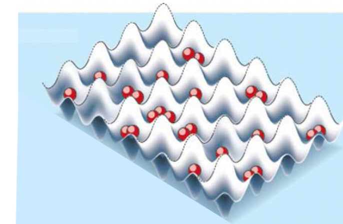

experiment with ultracold atoms in optical lattice

simulation by worm algorithm

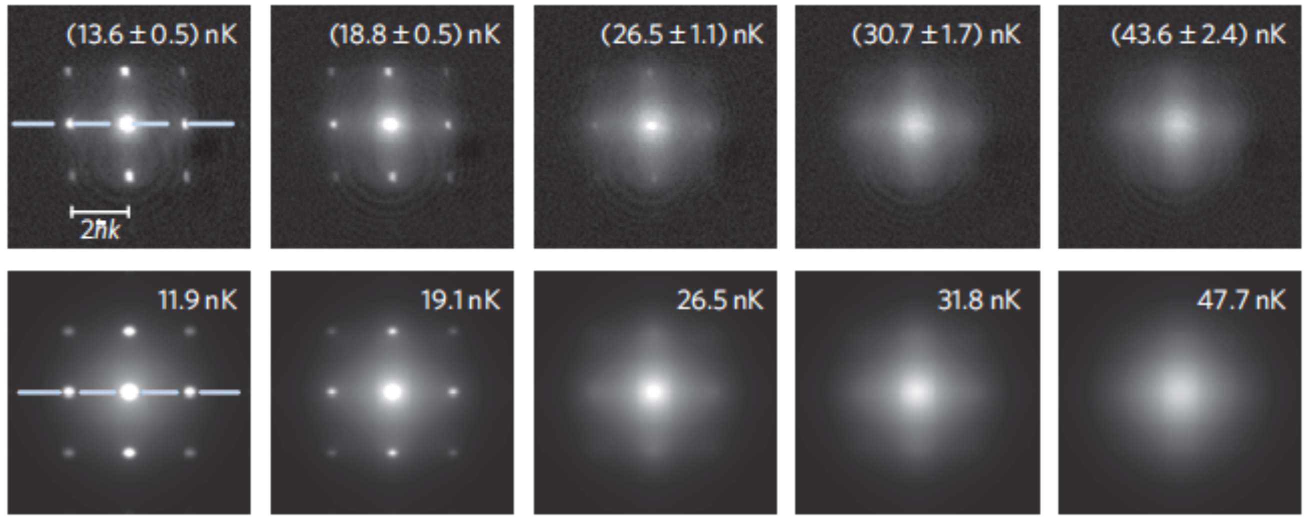

ARTICLES
nature physics
PUBLISHED ONLINE: 3 OCTOBER 2010 | DOI:10.1038/NPHYS1799

Suppression of the critical temperature for superfluidity near the Mott transition

S. Trotzky[1★†], L. Pollet[2,3†], F. Gerbier[4], U. Schnorrberger[1], I. Bloch[1,5], N. V. Prokof'ev[2,6], B. Svistunov[2,6] and M. Troyer[3]

Bose Hubbard model with bounded disorder at a commensurate filling

$$H = -t\sum_{\langle i,j\rangle} a_i^+ a_j + \frac{U}{2}\sum_i n_i(n_i - 1) + \sum_i \varepsilon_i n_i$$

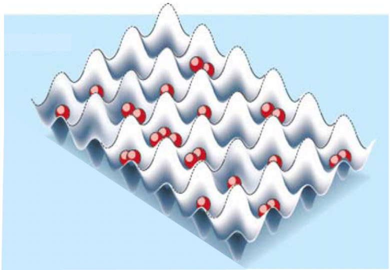

$\varepsilon_i \in [-\Delta, \Delta]$ random on-site potential

$\nu \equiv \bar{n}_i = 1$ (or other integer)

Superfluid (SF)

Mott insulator (MI) gapped insulator

Bose glass (BG) compressible insulator

T. Giamarchi and H.J. Schulz, Europhys. Lett. **3**, 1287 (1987).

M.P.A. Fisher, P.B. Weichman, G. Grinstein, and D.S. Fisher, Phys. Rev. B **40**, 546 (1989).

Q1: *Does disorder change the phase diagram at* $\Delta \ll U, t$?

Q2: *Is disorder a relevant perturbation for SF-insulator transition?*

3D and 2D: Essentially complete theoretical control

(Theorem of inclusions + worm algorithm simulations)

3D

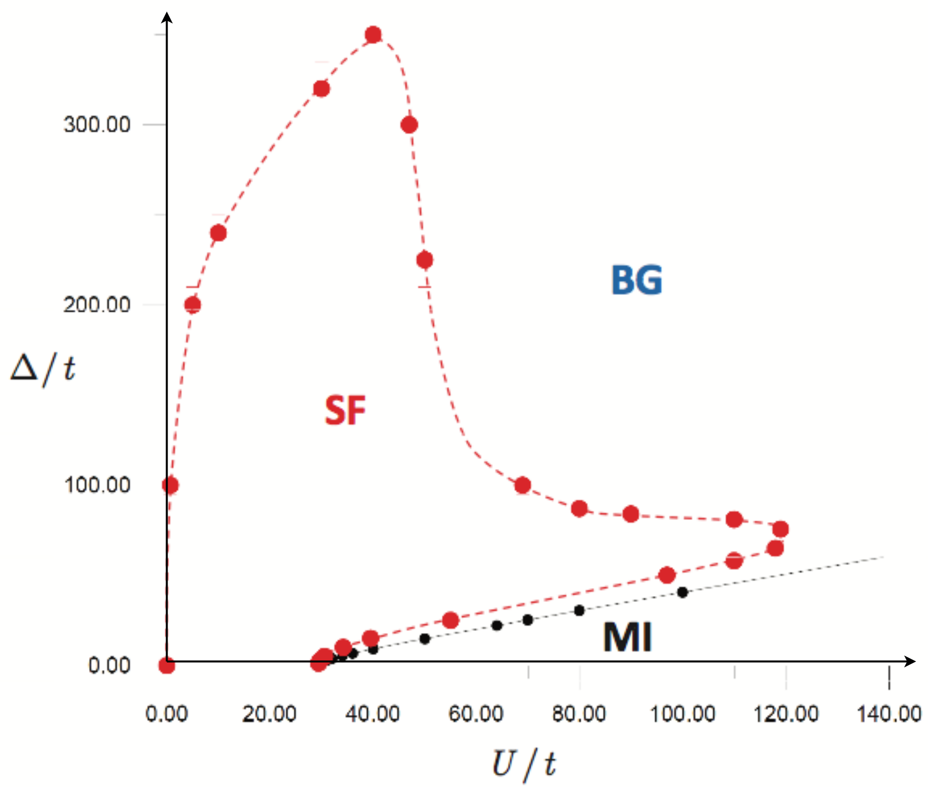

2D

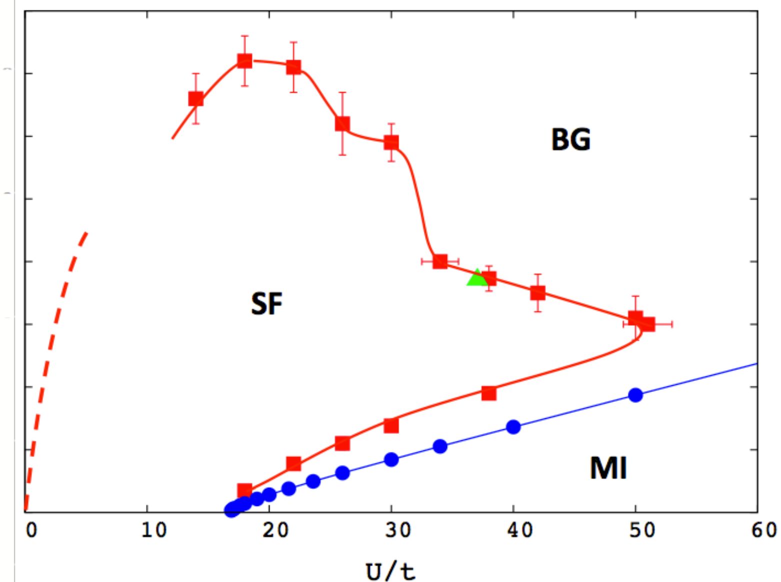

Gurarie, Pollet, Prokof'ev, Svistunov, and Troyer, PRB **80**, 214519 (2009)

Soyler, Kiselev, Prokof'ev, and Svistunov, PRL **107**, 185301 (2011)

1D case

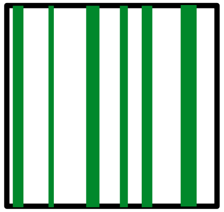

New universality class:
"scratched 2D XY."

Can preempt BKT-type transitions.

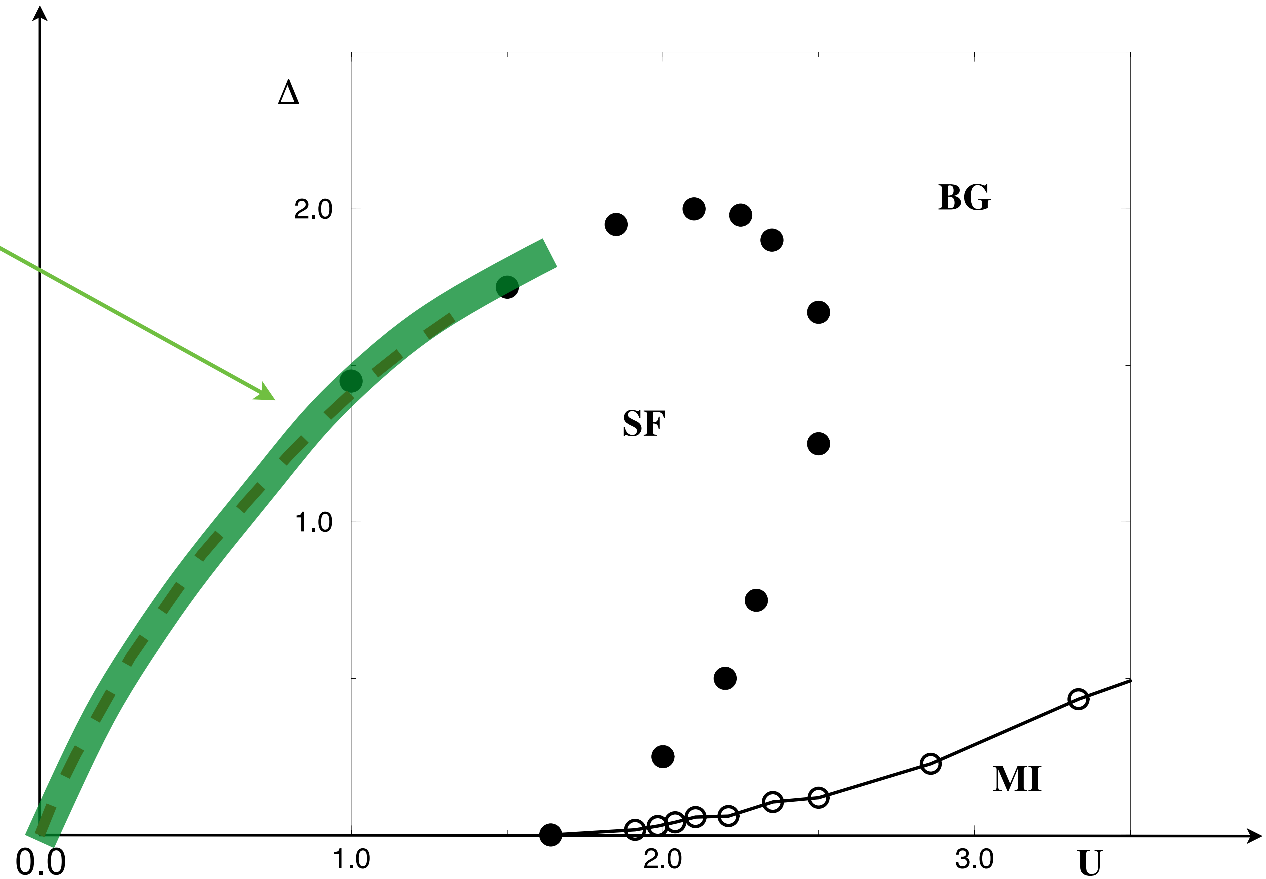

Pollet, Prokof'ev, and Svistunov, PRB **89**, 054204 (2014)

Yao, Pollet, Prokof'ev, and Svistunov, New J. Phys. **18**, 045018 (2016)

phase diagram: Prokof'ev and Svistunov (1998)

Bose Hubbard model: Emergent relativistic physics in the vicinity of the Mott transition

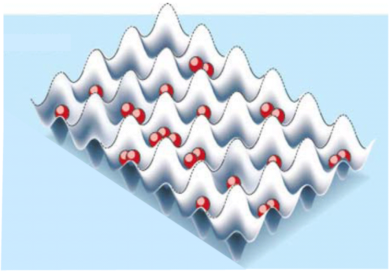

$$H = -t\sum_{\langle i,j\rangle} a_i^+ a_j + \frac{U}{2}\sum_i n_i\left(n_i - 1\right) \qquad \nu \equiv \bar{n}_i = 1$$

Emergence of particle-hole symmetry on the approach to the critical point from the Mott-insulator side

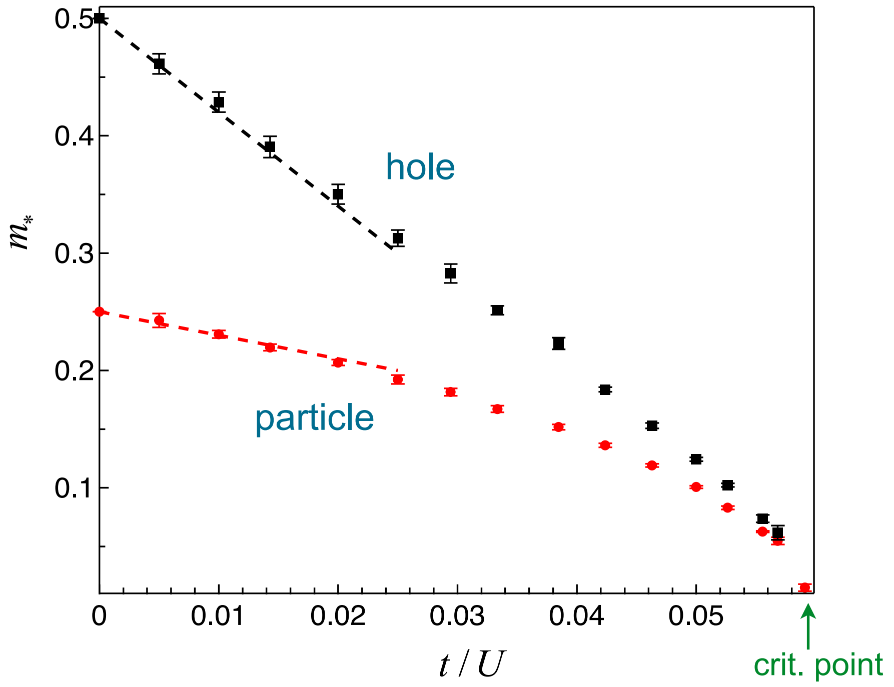

2D

Capogrosso-Sansone, Soyler, Prokof'ev, and Svistunov, Phys. Rev. A **77**, 015602 (2008)

The Halon: a quasiparticle featuring critical charge fractionalization

A static impurity in O(2) Wilson-Fisher conformal field theory in (2+1)

By particle-vortex duality, the theory also describes the net magnetic flux induced by a solenoid introduced into 3D superconductor at the critical temperature.

size of the halo: $r_0 \sim |V - V_c|^{-\tilde{\nu}}, \qquad \tilde{\nu} = 2.33(5)$

The halo charge $\pm 1/2$ is guaranteed by emergent particle-hole symmetry.

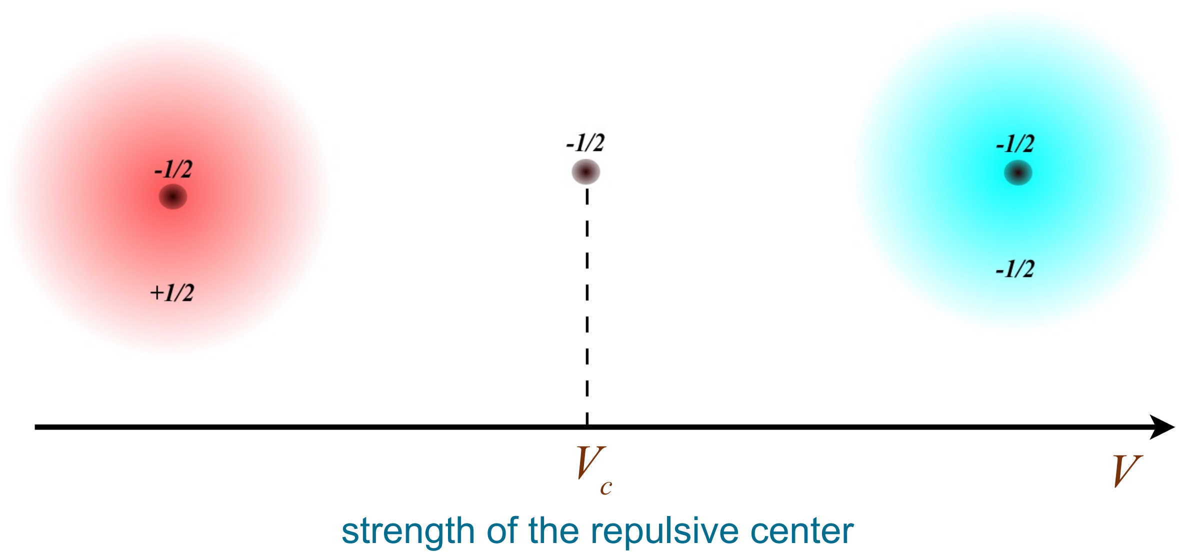

Huang, Chen, Deng, and Svistunov, PRB **94**, 220502(R) (2016); see also PRB 98, 214516 (2018) and PRB 98, 140503(R) (2018).